Supporting Information

Cr^{3+}-Induced Broadband Near-infrared I Combined with Near-infrared II Emission via Rare Earth Co-Doping in $Cs_2NaInCl_6$ for Multifunctional Detection

Hui Xie[a,b], Hui Fu[b], Zhentao Du[a]*, Linjie Tong[a,b], Jinliang Jiang[b], Xue Jiang[c], Jialong Zhao[c], Weiyou Yang[b], and Jinju Zheng[b]**

[a] School of Resources, Environment and Materials, Guangxi University, Nanning 530004, China

[b] Institute of Micro/Nano Materials and Devices, Ningbo University of Technology, Ningbo 315211, China

[c] School of Physical Science and Technology, MOE Key Laboratory of New Processing Technology for Non-ferrous Metals and Materials, Guangxi University, Nanning 530004, China

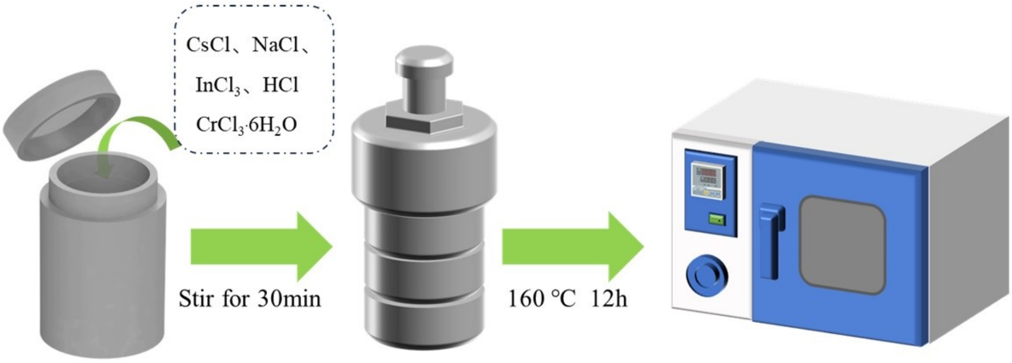

Figure S1. Schematic diagram of the hydrothermal synthesis for the samples.

Table S1. The ICP-OES data of Cr^{3+} doped CNIC DPs. The feeding ratios are determined based on the equation of [Cr]/[In]×100% and the actual doping concentrations are [Cr]/([In]+[Cr])×100%.

Samples	Feeding ratio [%]	Actual content [%]
	Cr^{3+}	Cr^{3+}
CNIC: Cr^{3+}	10	0.21
	20	0.34
	30	0.58
	40	1.15
	50	2.90

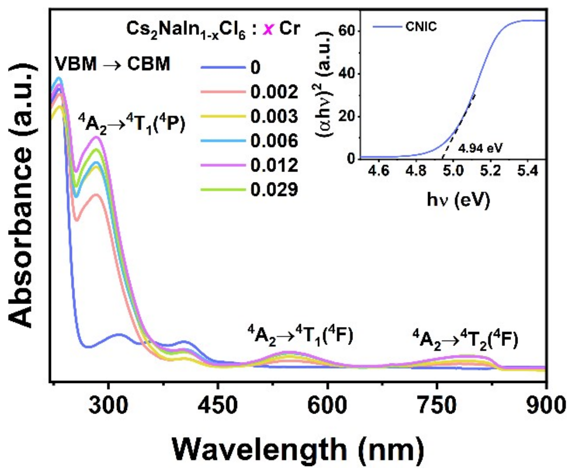

Figure S2. Absorption spectra of CNIC: Cr^{3+} with different Cr^{3+} doping concentrations.

Table S2. A summary of the NIR emission performance of different materials.

Samples	λ_{ex} [nm]	λ_{em} [nm]	FWHM [nm]	PLQY [%]	Themal stability	Ref.
K_2LiGaF_6: Cr^{3+}	430	766	133	82.5	$I_{425\ K}$ = 85%	1
$Cs_2AgInCl_6$: Cr^{3+}/Mn^{2+}	350	1000	188	49.3	/	2
$Cs_2NaScCl_6$: Cr^{3+}	300	950	162	100	$I_{423\ K\text{-}20\ h}$ = 91.9%	3
$Cs_2AgInCl_6$: Cr^{3+}/Er^{3+}	360/583/815	1010/1540	162	57.5	$I_{423\ K\text{-}960\ h}$ = 85%	4
$MgTiO_3$:Cr^{3+}	514	866	154	31.55	$I_{350\ K}$ = 40%	5
Cs_2TeCl_6:Cr^{3+}	380	590	~100	81.5	$I_{473\ K\text{-}1h}$ = 87% $I_{373\ K\text{-}1h}$ = 94%	6
$Ca_{0.5}Cd_{0.5}Ti_4(PO_4)_6$: Cr^{3+}	470	832	165	46.63	$I_{373\ K}$ = 43.48%	7
$Sr_2ScTa_{0.6}Nb_{0.4}O_6$: Cr^{3+}	337	954	179.7	86.3	$I_{373\ K}$ = 54%	8
Cs_2SnCl_6: W^{4+}	365	965	~130	/	$I_{300\ K}$ = 64%	9
$CaLaMgSbO_6$: Ni^{2+}	440	1546	229	32.94	$I_{373\ K}$ = 40%	10
Sr_2ScTaO_6: Ni^{2+}	420	1441	254	49.23	$I_{373\ K}$ = 45.65%	11
$ZnAl_2O_4$: Mn^{2+}	450	830	135	85.8	$I_{423\ K}$ = 60%	12
$Li_5La_3Sb_2O_{12}$: Mn^{4+}	341	709	~50	56.3	$I_{423\ K}$ = 54.7%	13
$Ca_3Sn_2Ga_2GeO_{12}$: Fe^{3+}	278/406	760	~80	54.1	$I_{423\ K}$ = 72%	14
$Cs_2NaLuCl_6$: Fe^{3+}	395	1265	309	17.29	$I_{373\ K}$ = 23.35%	15
$NaBaScSi_2O_7$: Fe^{3+}	301	815	116	16.2	$I_{423\ K}$ = 46%	16
$Cs_2NaInCl_6$: Cr^{3+}	290	960	160	92.41	$I_{423\ K\text{-}480\ h}$ = 87% $I_{340\ K}$= 50%	**This work**

Note: I_T refers to the ratio of the emission intensity at a certain temperature T to that at the initial temperature.

Table S3. The ICP-OES data of Cr^{3+}/Ho^{3+} doped CNIC DPs. The feeding ratios are determined based on the equation of [Cr]/[In]×100% and [Ho]/[In]×100%, while the actual doping contents are determined by [Cr]/([In]+[Cr]+[Ho])×100% and [Ho]/([In]+[Cr]+[Ho])×100%.

Sample	Feeding ratio [%]		Actual content [%]	
	Cr^{3+}	Ho^{3+}	Cr^{3+}	Ho^{3+}
CNIC: Cr^{3+}/Ho^{3+}	40	20	0.99	0.61
	40	40	1.12	1.77
	40	80	0.89	2.99
	40	100	0.71	4.0
	40	120	0.34	7.78

Table S4. The ICP-OES data of Cr^{3+}/Tm^{3+} doped CNIC DPs. The feeding ratios are determined based on the equation of [Cr]/[In]×100% and [Tm]/[In]×100%, while the actual doping contents are determined by [Cr]/([In]+[Cr]+[Tm])×100% and [Tm]/([In]+[Cr]+[Tm])×100%.

Sample	Feeding ratio [%]		Actual content [%]	
	Cr^{3+}	Tm^{3+}	Cr^{3+}	Tm^{3+}
CNIC: Cr^{3+}/Tm^{3+}	40	20	0.90	0.58
	40	40	1.32	0.99
	40	80	1.18	1.52
	40	100	0.87	1.88
	40	120	0.43	2.93

Table S5. The ICP-OES data of Cr^{3+}/Er^{3+} doped CNIC DPs. The feeding ratios are determined based on the equation of [Cr]/[In]×100% and [Er]/[In]×100%, while the actual doping contents are determined by [Cr]/([In]+[Cr]+[Er])×100% and [Er]/([In]+[Cr]+[Er])×100%.

Sample	Feeding ratio [%]		Actual content [%]	
	Cr^{3+}	Er^{3+}	Cr^{3+}	Er^{3+}
CNIC: Cr^{3+}/Er^{3+}	40	20	1.02	0.32
	40	40	1.16	0.89
	40	80	0.98	1.86
	40	100	0.81	2.69
	40	120	0.44	4.16

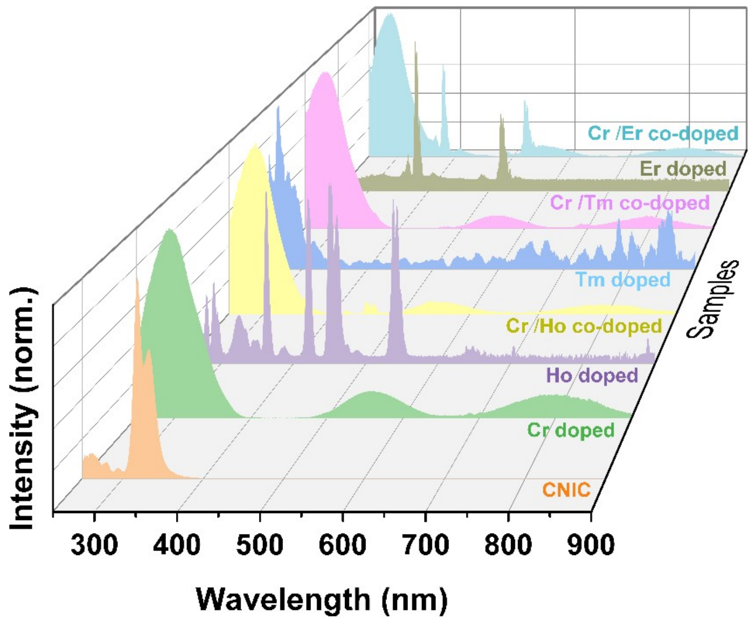

Figure S3. PLE spectra of CNIC (λ_{em}= 445 nm), CNIC: Cr^{3+} (λ_{em}= 960 nm), CNIC: Ho^{3+} (λ_{em}= 1180 nm), CNIC: Ho^{3+} (λ_{em}= 1180 nm), CNIC: Tm^{3+} (λ_{em}= 1220 nm), CNIC: Cr^{3+}, Tm^{3+} (λ_{em}= 1220 nm), CNIC: Er^{3+} (λ_{em}= 1540 nm) and CNIC: Cr^{3+}, Er^{3+} (λ_{em}= 1540 nm).

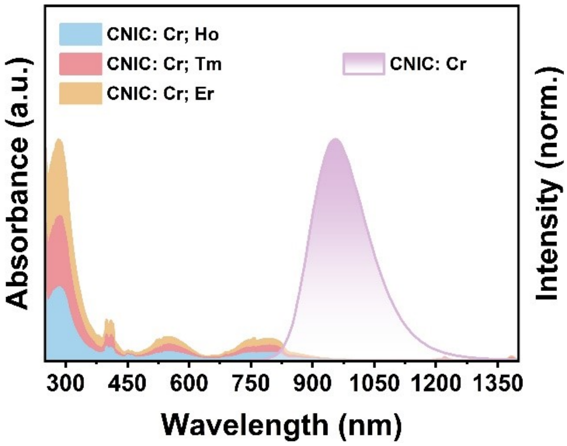

Figure S4. The absorption spectra of CNIC: Cr^{3+}, Ln^{3+} (Ln^{3+} = Ho^{3+}, Tm^{3+}, Er^{3+}) and the emission of CNIC: Cr^{3+} under 290 nm excitation.

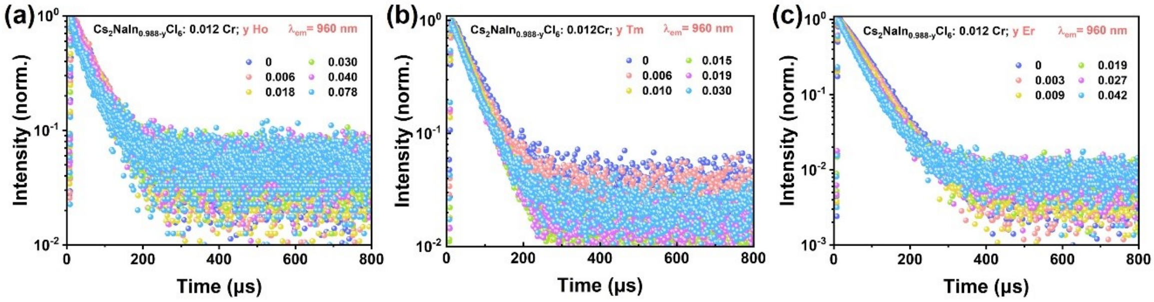

Figure S5. NIR PL decay curves at 960 nm of $Cs_2NaIn_{0.988\text{-}y}Cl_6$: 0.012 Cr^{3+}, *y* Ln^{3+} (Ln^{3+} = Ho^{3+}, Tm^{3+}, Er^{3+}) under 290 nm excitation.

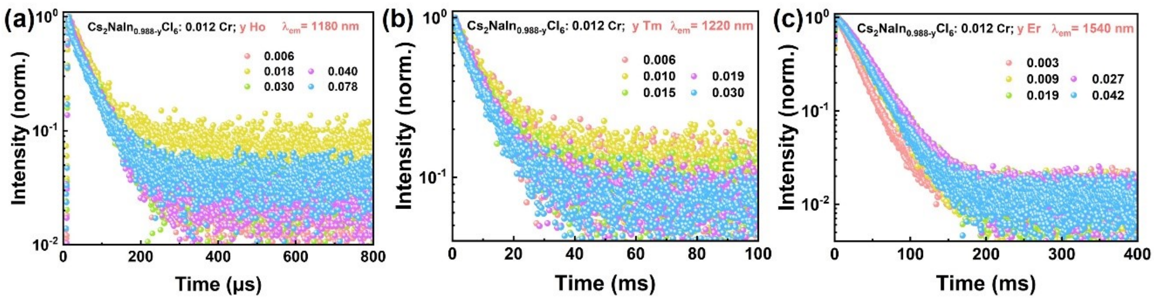

Figure S6. NIR PL decay curves of $Cs_2NaIn_{0.988\text{-}y}Cl_6$: 0.012 Cr^{3+}, *y* Ho^{3+} (λ_{em}= 1180 nm), $Cs_2NaIn_{0.988\text{-}y}Cl_6$: 0.012 Cr^{3+}, *y* Tm^{3+} (λ_{em}= 1220 nm), $Cs_2NaIn_{0.988\text{-}y}Cl_6$: 0.012 Cr^{3+}, *y* Er^{3+} (λ_{em}= 1540 nm) under 290 nm excitation.

Table S6. Decay lifetimes (τ) and energy-transfer efficiency (η_{ET}) of $Cs_2NaIn_{0.988-y}Cl_6$: 0.012 Cr^{3+}, y Ho^{3+} under 290 nm excitation.

Samples	τ [μs] (λ_{em}=960 nm)	τ [μs] (λ_{em}=1180 nm)	η_{ET} [%]
0%	56.01		
20%	53.58	55.71	4.3%
40%	50.15	53.05	10.5%
80%	49.06	52.33	12.4%
100%	48.55	51.45	13.3%
120%	47.8	48.89	14.7%

Table S7. Decay lifetimes (τ) and energy-transfer efficiency (η_{ET}) of $Cs_2NaIn_{0.988-y}Cl_6$: 0.012 Cr^{3+}, y Tm^{3+} under 290 nm excitation.

Samples	τ [μs] (λ_{em}=960 nm)	τ [μs] (λ_{em}=1220 nm)	η_{ET} [%]
0%	56.01	-	-
20%	51.62	9.74	7.8%
40%	49.66	9.99	11.3%
80%	47.51	9.24	15.1%
100%	47.20	9.09	15.7%
120%	46.77	8.34	16.5%

Table S8. Decay lifetimes (τ) and energy-transfer efficiency (η_{ET}) of $Cs_2NaIn_{0.988-y}Cl_6$: 0.012 Cr^{3+}, y Er^{3+} under 290 nm excitation.

Samples	τ [μs] (λ_{em}=960 nm)	τ [μs] (λ_{em}=1540 nm)	η_{ET} [%]
0%	56.01	-	-
20%	54.77	23.46	2.2%
40%	51.61	29.89	7.9%
80%	49.10	32.15	12.3%
100%	48.79	31.64	12.9%
120%	46.62	30.13	16.8%

Note: the equation of ET efficiency (η_{ET}) is as follow:

$$\eta_{ET} = 1 - \frac{\tau_x}{\tau_0} \tag{1}$$

where τ_0 and τ_x are the decay lifetimes monitored at 960 nm in the Cr^{3+} singly-doped DPs and the Cr^{3+}/Ln^{3+} co-doped DPs, respectively.

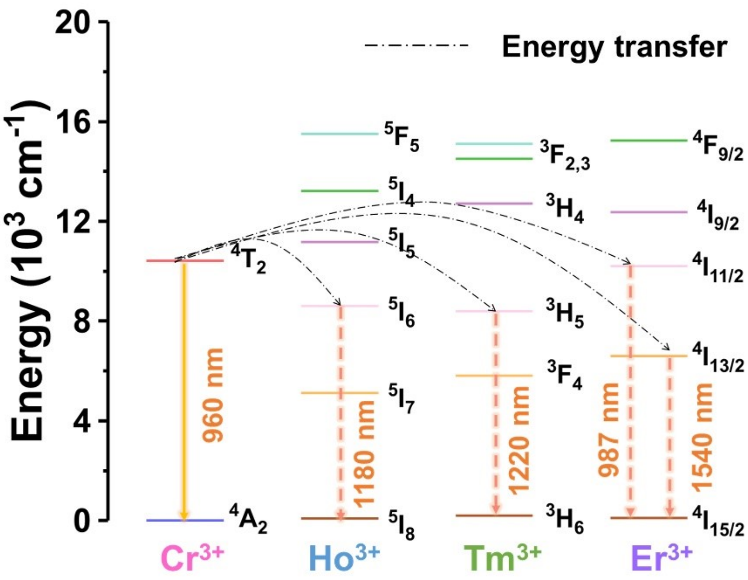

Figure S7. Schematic diagram of the photophysical process of energy transfer from Cr^{3+} to Ln^{3+} in CNIC: Cr^{3+}/Ln^{3+} (Ln^{3+} = Ho^{3+}, Tm^{3+}, Er^{3+}).

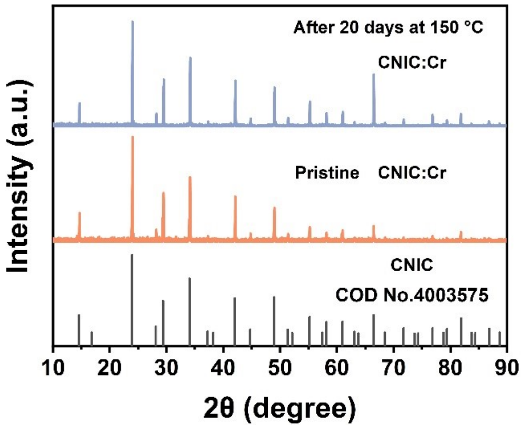

Figure S8. XRD patterns of CNIC: Cr^{3+} after heating at 150 °C for 20 days.

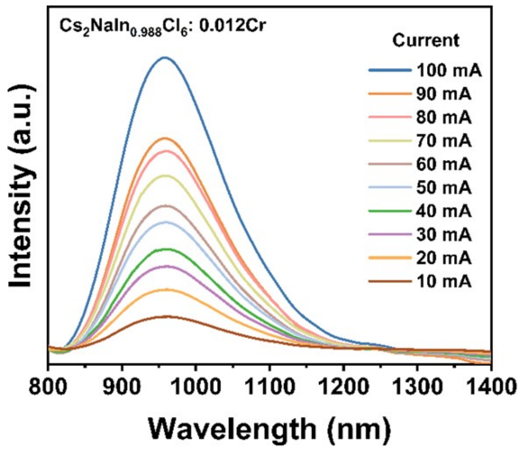

Figure S9. EL spectra of the fabricated NIR pc-LED measured under a voltage of 24V and varying driving currents from 10 mA to 100 mA.

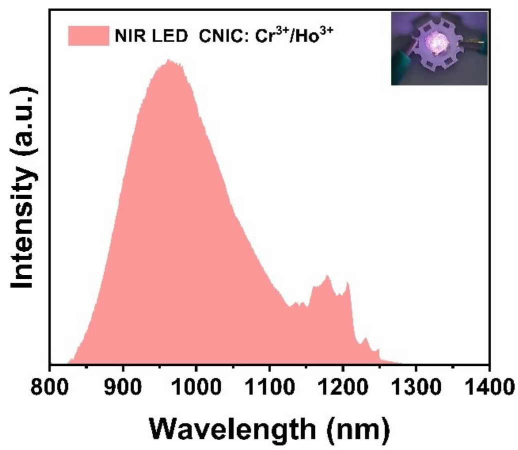

Figure S10. Emission spectrum of the LED fabricated by CNIC: Cr^{3+} /Ho^{3+} DPs under 310 nm chip excitation.

References

1. Y. Li, J. Zuo, T. Zheng, S. Yang, P. He, J. Zhang, S. Liu, F. Yang, J. Peng and X. Ye, *Adv. Opt. Mater.*, 2024, **12**, 2400171.
2. D. Chen, C. Wu, H. Li, L. Zhou, P. Chen, Q. Pang, X. Zhang and J. Z. Zhang, *J. Mater. Chem. C*, 2023, **11**, 12649-12657.
3. C. Zhao, Y. Gao, J. Wang and J. Qiu, *Laser Photonics Rev.*, 2023, **18**, 2300952.
4. W. Gan, L. Cao, S. Gu, H. Lian, Z. Xia and J. Wang, *Chem. Mater.*, 2023, **35**, 5291-5299.
5. Y. Wang, C. Deng, J. Zhang, Y. Liu, J. Chen, Y. Jin, Z. Fan and D. Fan, *Ceram. Int.*, 2025, **51**, 15466-15474.
6. L. Zi, W. Xu, Z. Song, R. Sun, S. Liu, T. Xie, J. Zhu, S. Lu and H. Song, *J. Mater. Chem. C*, 2023, **11**, 2695-2702.
7. B. Yan, J. Wen, Y. Zhou, Q. Sha, X. Huang, Z. Dong, C. Wang, Q. Wang, L. Ning and C.-K. Duan, *Ceram. Int.*, 2025, **51**, 11018-11025.
8. M. Han, Z. Gao, Y. Zhang, S. Chen, J. Li, Y. Shen, Y. Tian and D. Deng, *J. Alloys Compd.*, 2024, **995**, 174780.
9. B. Mondal, S. Mehta, A. Mondal and A. Nag, *J Phys Chem Lett*, 2025, **16**, 4937-4943.
10. W. Wang, S. Su, H. Xu, W. Yang, L. Zhao, W. Teng, X. Yang, X. Sun, H. Zhang, J. Cui, Y. Zhang, B. Teng and D. Zhong, *J. Lumin.*, 2025, **282**, 121237.
11. F. Huang, Y. Yan, G. Zhu, S. Zhao, H. Wang, D. Deng, S. Xu and H. Yu, *Appl. Mater. Today*, 2025, **44**, 102731.
12. C. Zhan, H. Zhu, S. Liang, W. Nie, Z. Wang and M. Hong, *Adv. Opt. Mater.*, 2024, **12**, 2400574.
13. B. Han, L. Shi, Y. Lv, W. Li, J. Hu, Y. Liu, Y. Wang and X. Chen, *Ceram. Int.*, 2025, DOI: 10.1016/j.ceramint.2025.05.331.
14. P. Wang, A. Chen, B. Lou, Q. Chen, D. Zhang, C. K. Duan and C. G. Ma, *Laser Photonics Rev.*, 2025, e00030.
15. F. Zhu, Y. Gao and J. Qiu, *Adv. Opt. Mater.*, 2025, 2500549.
16. C. Gong, Z. Wang, J. Wang, X. Xue and X. Wang, *Sci. China Mater.*, 2025, **68**, 1074-1081.